Procedia Manufacturing
Volume 5, 2016, Pages 644–657
44th Proceedings of the North American Manufacturing Research Institution of SME http://www.sme.org/namrc

A Preliminary Machinability Study of Flake and Compacted Graphite Irons with Multilayer Coated and Uncoated Carbide Inserts

Sirisak Tooptong[1], Kyung-Hee Park[2] , Seok-Woo Lee[2] and Patrick Y. Kwon[1*]
[1]*Michigan State University, East Lansing, USA*
[2]*KITECH, Cheonan-si, Republic of Korea*
*tooptong@msu.edu, *pkwon@egr.msu.edu*

Abstract
Compacted graphite iron (CGI) is considered to be one of the most promising materials for many automotive applications and has adopted by some automotive companies. Comparing to widely used flake graphite iron (FGI), CGI has superior physical and mechanical properties. The main drawback of this material is known to be its poor machinability. A preliminary study on flank and crater wear was conducted by dry turning experiments with both FGI and CGI using uncoated WC tools and multilayer coated tools. Confocal Laser Scanning Microscopy (CLSM) was used to investigate worn areas of the cutting tools. Despite of the reported poor machinability of CGI, our turning experiments showed that both flank and crater wear were higher for FGI compared to CGI when using uncoated WC tools at the cutting speed of 150, 250 and 350 m/min. An unexpected adhesion layer on the flank side of carbide inserts was observed when turning CGI, which believe to protect the flank surface and reduce flank wear. The adhesion on rake face concentrated on the cutting edge when turning CGI while the sporadic attachments of work materials are observed throughout the rake interface with FGI. In contrast, no adhesion layer was presented when both FGI and CGI were turned using multilayer coated tools, which yielded more flank and crater wear when turning CGI.

Keywords: CGI, FGI, Machinability, Tool-wear, WC tool, straight turning, CLSM

1 Introduction

Generally two main characteristics of a cast iron affect its mechanical properties and machinability. The first characteristic is graphite morphology. As illustrated in Figure 1, Flake Graphite Iron (FGI) has lamellar or flak graphite, which acts as a very effective stress risers (Shen-Chih and Yin-Bean 1991). Compacted Graphite Iron (CGI) has a cloud, worm or vermicular graphite shape, which

Selection and peer-review under responsibility of the Scientific Programme Committee of NAMRI/SME

doi:10.1016/j.promfg.2016.08.053

reduces the effect of the stress risers to strengthen mechanical properties. Even though not considered in this paper, nodular graphite iron (NGI) has a graphite shape of isolated spheroids or nodules and provides even better ductility and higher strength. The second characteristic of a cast iron is the ratio between ferrite and pearlite phase in the metallic matrix.

CGI was established in 1949 around the same time as FGI and NGI (Dawson and Schroeder 2004). FGI were widely used since then because of the better machinability comparing to the other two cast irons. About few decades ago, many researchers and industry especially in automotive field were looking back to CGI due to its superior physical and mechanical properties required in many critical applications where high strength per weight ratio is critical. When these cast irons are examined, the CGI offers the mechanical properties in between FGI and NGI as shown in Table 1 with at least 75% higher strength, 40% higher elastic modulus compared to FGI and not as quite high as those of NGI. (Dawson et al., 2001)

Property	FGI	CGI	NGI
Tensile strength (MPa)	250	452	750
Elastic modulus (GPa)	105	145	160
Elongation (%)	0	1.5	5
Thermal conductivity (W/(m.K))	48	37	28
Hardness (BHN 10/3000)	179-202	217-241	217-255

Table 1: Typical material physical properties of FGI, CGI, NGI (Dawson et. al. 2001)

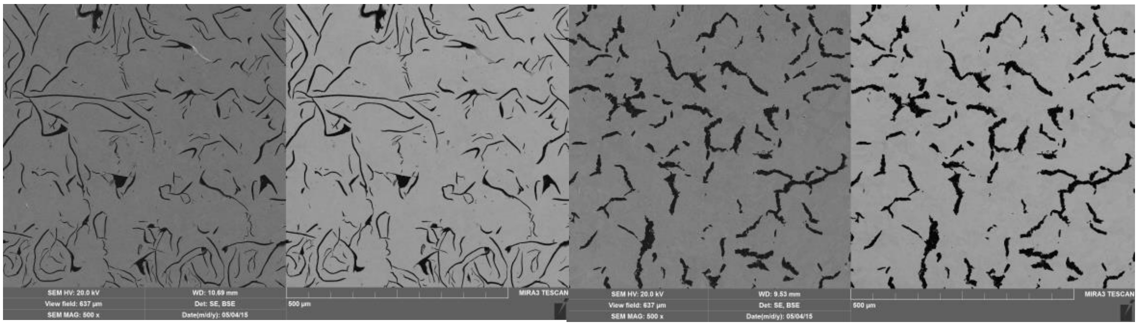

(a) (b)

Figure 1: Microstructure of FGI (a) and CGI (b) observed in SEM.

Phillip (1981) first reported the experiments on FGI, CGI and NGI with distinct matrix phases, considered to be either ferritic or pearlitic, by continuously turning with uncoated carbide, coated carbide and Al_2O_3 tools. The experiment showed that uncoated carbide inserts provided better performance than other tools when the cutting speed is less than 125m/min. The machinability of CGI was in between those of FGI and NGI (Philip 1981). A similar conclusion on the machinability of CGI compared to other cast irons also reported by Lalich and LaPresta (1977) and Oathout (1978).

Dawson (1999) introduced the important characteristics of cast iron influencing the machinability, graphite shape, pearlite content, chemical elements and inclusion effects:. In another study by Dawson et al. (2001), the PCBN tool life dropped as the graphite shape changed from a fully flake shape to a 50/50 flake/compacted shape and gradually decreased until the graphite shape became nodule. Nayyar et al. (2013) stated that tool life was depended on the microstructure and mechanical properties of the FGI and CGI materials. The improvement in ultimate tensile strength, hardness, and percentage of nodularity of CGI also decreased tool life. Using coated carbide inserts, turning tests at 300 m/min. showed that tool life for FGI is at least double that of CGI. Again, Dawson et al. (2001) carried out the turning experiments for CGI with various pearlite contents and FGI using carbide tools at the cutting speeds of 150 and 250 m/min. At 250 m/min, the tool life of coated carbide tool did not show any significant drop for the pearlite range between 75% and 97.5%. On the other hand, at 150 m/min tool life gradually decreased at this pearlite range. At 150 m/min, machining of CGI reduced the tool life by one third and when cutting CGI at 250 m/min, tool life dropped by 80% compared to FGI. Mocellin et al. (2004) reported that tool life was dropped to 44% when CGI with 100% pearlite was manufactured compared to FGI (FC-250) in drilling operation. Nayyar et al. (2013) also confirmed that tool life decreased as the amount of pearlite increased. Berglund et al. (2009) concluded that more flank wear was observed with the presence of high pearlite content. Tool life was not significantly affected by the interlamellar distance of pearlite. For milling, pearlite content in CGI strongly affected the tool life.

Dawson (2001) summarized the effect of Cu, Sn, Mn, Sb as pearlite stabilizing elements. Mn stabilized pearlite content to 100% which decreasing the wear of coated carbide tools by 50-100%. Sb was used to increase the pearlite content from 97.5% to 99% and provided slightly better tool life at the low cutting speed when coated carbide tools were used. CGI was stable at low sulfur content typically around 0.005-0.025%. PCBN turning experiments showed that machinability of FGI decreased when the sulfur content decreased. Carbide turning test indicated that slightly increasing of Ti at the trace level could reduce tool life about 50%.

Abele et al. (2002) conducted straight turning using coated carbide, ceramic and CBN tools on FGI, CGI with low pearlite and CGI with high pearlite and concluded that when using the coated carbide tools at low cutting speed (around 100 to 120 m/min), tool life is acceptable for all three cast irons. At high cutting speed (around 250m/min), the tool life for CGI coated carbides was substantially reduced. When CBN tools were used at high cutting speed (above 400m/min), tool life decreased by a factor of 10 to 20. Gestel et al. (2000) mentioned that MnS layer which formed on the inserts when cutting FGI at high cutting speed led to significant difference in machinability between FGI and CGI. Heck et al. (2008) had reported the difficulty of continuous turning at high cutting speed for CGI due to the absence of a self lubricating and protection layer of MnS. Pereira et al. (2006) conducted the turning operations of FGI (FC25) with uncoated carbide tools at 100, 150, 200m/min and reported that the percentage area occupied by MnS inclusion played important role in the machinability of FGI. The influence of the MnS had a significant effect at higher cutting speeds. Moreover, Nayyar et al. (2012) also report that dry continuous turning of FGI provided almost 10 times of the tool life compared to CGI at 300m/min with coated carbide inserts.

The formation of MnS layer is contributed to the excellent machinability of FGI at the extremely high cutting speeds only possible for PCBN tools. This layer cannot be formed at the cutting speeds normally used for carbide tools. In this paper, we conducted straight turning experiments to understand flank and crater wear in the range of the cutting speeds typically used with carbide inserts. This paper intends to find the reason behind the poor machinability of CGI with the uncoated and coated carbide inserts.

2 Experimental Procedures

2.1 Workpiece Materials

Solid bars of pearlitic FGI (FC-250) was obtained from Alro Steel Company (Lansing, MI) while the tubular CGI (GJV 450) bars with one end closed was obtained from Sintercast AB (Katrineholm, Sweden). According to Sintercast, GJV450 is known to have the 95% pearlitic structure. The dimensions and chemical composition of each cast iron are shown in Table 2 and Table 3, respectively. The chemical compositions for each iron in Table 3 were provided by each respective supplier. Between FGI and CGI, the content of Mn is substantially reduced on CGI, which is the necessary condition to form CGI (Dawson et al., 2001). With the substantial amount of Mn and S in FGI, MnS is formed, which are known to help machining FGI. Mg was added to CGI to form vermicular graphite, the essential characteristic of CGI. Mg also has much higher reaction potential with S than Mn. Hence, in CGI, MgS is formed, which exists as the abrasive in metal cutting. (Gastel et al., 2000). Before conducting the turning experiments, the exterior surfaces of all test specimens were cut to eliminate any surface oxidation layer.

Work material	Type	Outer diameter (mm)	Inner diameter (mm)	Length (mm)
FGI	Solid bar	152.4	-	254
CGI	Cylinder	145	98	204

Table 2: The Dimensions of Our Cast Iron Work Materials.

	%C	%Si	%Mn	%S	%Cr	%Cu	%Mg	%Sn	%P	%Ti
FGI	3.010	2.42	0.73	0.055	Resid.	Resid.	-	Resid.	0.027	-
CGI	3.55	2.22	0.39	0.007	0.029	0.94	0.011	0.081	-	0.006

Table 3: Chemical composition of Our Cast Iron Work materials

2.2 Experimental evaluation

Uncoated carbide (WC +6% Co) inserts manufactured by Sanvik with the reference SCMW 120408 H13A and the tool holder of the reference SSBCR 2525M 12 were used. According to the specification of the tool holder, the rake angle of 0 degree, tool cutting edge angle of 75 degree and tool lead angle of 15 degree were used. Multilayer coated carbides also manufactured by Sanvik with the reference SNMA 12 04 08 KR 3205 and 3210 (Inserts information is shown in Table 4.) with tool holder of the reference DSBNR 2020K12 were used with the rake angle of -6 degree, the tool cutting edge angle of 75 degree and the tool lead angle of 15 degree. Both Sandvik 3205 and 3210 inserts were coated in two layers, Ti(C,N) and Al_2O_3 (exterior coating) and the flank surface had additional thin (1-2 microns) TiN coating.

To investigate the wear characteristic of these inserts, straight turning of cast iron specimens were conducted. Both FGI and CGI were machined at various cutting speed 150 m/min, 250 m/min, and 350 m/min for uncoated carbide inserts and only 250 m/min for multilayer coated carbide inserts. The feed rate and depth of cut were held constant at 0.2 mm/rev and 2 mm, respectively. Turning was carried out until the inserts were gradually worn down to average and maximum flank wear 300 and 600 microns, respectively, defined by ISO 3685. Turning was interrupted sporadically to retrieve the wear profile from each insert corner in order to attain the wear evolution. After each interruption, a fresh corner of an insert was used. Daewoo Puma 300 L CNC lathe was used to carry the experiments. After machining, the inserts were etched by HCl solution to remove the built-up and adhesion of the workpiece materials. Both flank and rake surfaces were investigated carefully with a Confocal Laser Scanning Microscope (CLSM), a Scanning Electron Microscope (SEM, 6610LV) with Energy Dispersive X-ray (EDX).

Cutting Tool	Main Ingredient	%Co	Inner layer Ti(C,N) (μm)	Middle layer Al_2O_3 (μm)	Outer layer TiN (μm)
Carbide	WC	6	-	-	-
Sandvik 3205	WC	5	5	5	1-2
Sandvik 3210	WC	6	6-7	3-4	1-2

Table 4: Cutting Tool information (Two layers on crater surface in gray on each coated inserts).

3 Results

3.1 Frank Wear

Surprisingly, the machinability of CGI was better than FGI with uncoated carbide inserts. It was puzzling to observe the machinability CGI better than that of FGI. After the machining experiments, adhesion layers were completely covering the flank interface with work material when CGI was machined at least at the cutting speeds of 150 and 250m/min and some at the cutting speed of 350m/min as illustrated in Figure 2. When cutting FGI at the cutting speed of 150m/min, the adhesion layer was also formed at the beginning of the cutting process but quickly disappeared shortly after (within a minute or so of cutting). Flank wear is mostly have the characteristic scoring marks as presented in Figure 3 when turning FGI. For CGI, after the adhesion layer has been etched, we can observe the distinct damages on the flank surface as shown in Figure 7. With the adhesion layer, flank damage can be presented in two distinct patterns. Flank surface near the cutting edge has rough pattern due to the protruded carbide gains as shown in Figure 6(a) while the region away from the cutting edge may be the result of sliding wear, scratching wear caused by hard inclusions possibly from loose carbide grains. These are quite distinct from the scoring marks caused by the inhomogeneity in the microstructure as seen in Figure 7. The adhesion layer leads to the distinct flank wear damage not typically found in metal cutting. For CGI, the adhesion layers continue to exist for very long time (up to five minutes). However, the flank wear becomes eventually flank wear shown in Figure 7 as the inhomogeneities within the work material damage the cutting tools more locally by creating scoring marks. Thus, when the flank wear reaches the criteria defined by ISO 3685, both CGI and FGI produce the scoring marks on the flank surface. However, with the coated inserts, no adhesion layer seen on the uncoated inserts was observed either FGI or CGI. And perhaps more interestingly, with the coated inserts the machinability of CGI was worse than that of FGI as expected. Table 6 was constructed to summarize the flank wear.

In term of the chips generated, CGI forms discrete chips while FGI forms more continuous chips. Based on the chips attained, the cutting temperature when cutting FGI seems to be much higher than that of CGI under the same condition contradictory to the experiment carried out by Gastel et al. (1999). Definitely more deformation occurs on FGI during chip formation due the difference in microstructure as shown in Figures 4 and 5. Figure 4 and 5 show the optical images of chips after CGI and FGI were cut. As being observed, both CGI and FGI produced discontinuous/segmentation chips. From Figure 5(a), FGI chip color turned to purple indicating the oxidation occurred.

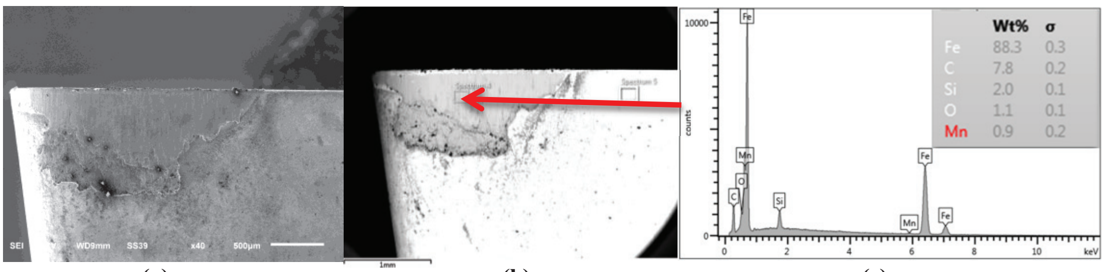

(a) **(b)** **(c)**

Figure 2: SEM and BSE images of uncoated insert after machining CGI at 150m/min for two mins with adhesion (a), (b), and EDS indicated that adhesion material was mainly Fe (c).

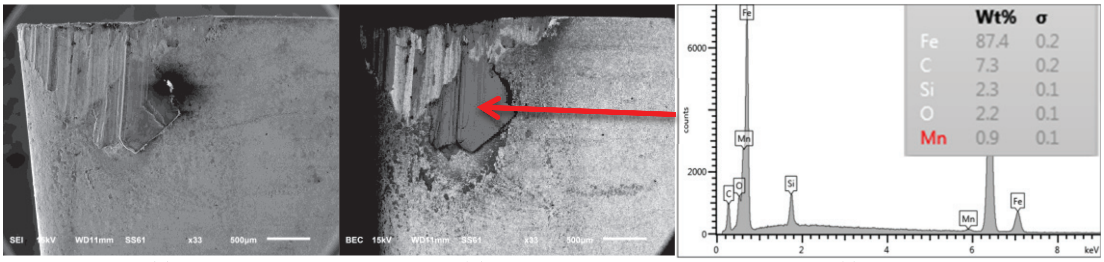

(a) **(b)** **(c)**

Figure 3: SEM and BSE images of uncoated insert after machining FGI at 250m/min for one min with adhesion (a), (b), and EDS indicated that adhesion material was mainly Fe (c).

	Uncoated carbide inserts	Multilayer coated carbide inserts
FGI	Some adhesion layer	No adhesion layer
CGI	Adhesion layer	No adhesion layer

Table 6: Formation of adhesion layer on cutting insert.

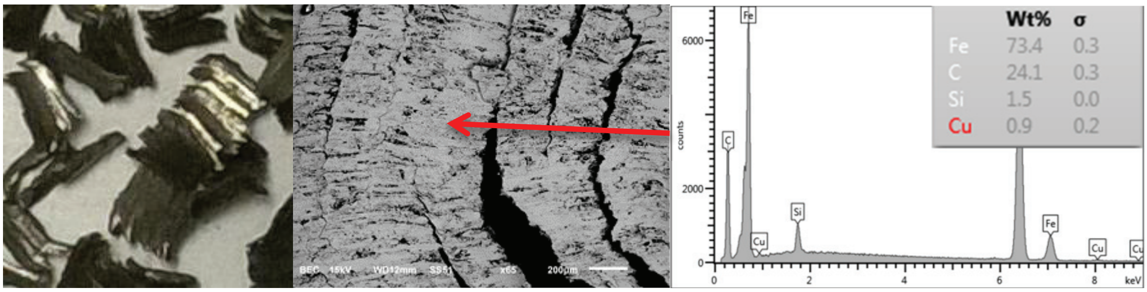

(a) **(b)** **(c)**

Figure 4: (a) optical image, (b) BSE image of chips produced under turning CGI with uncoated carbide insert at 350 m/min for one min., (c) EDS showed chemical composition of chips.

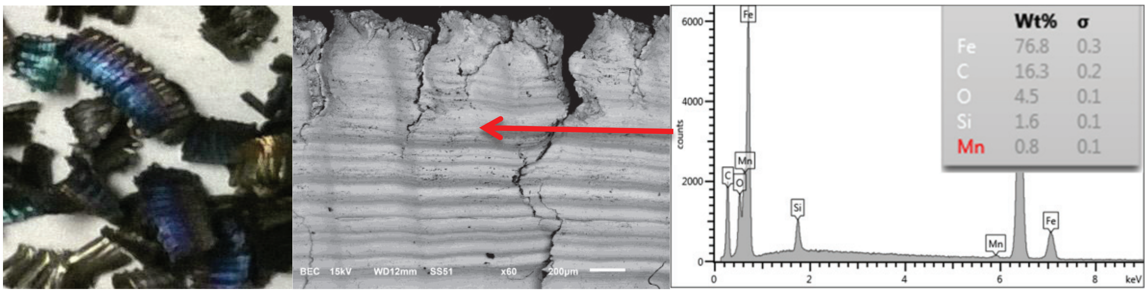

(a) **(b)** **(c)**

Figure 5: (a) optical image, (b) BSE image of chips produced under turning FGI with uncoated carbide insert at 350 m/min for one min., (c) EDS showed chemical composition of chips.

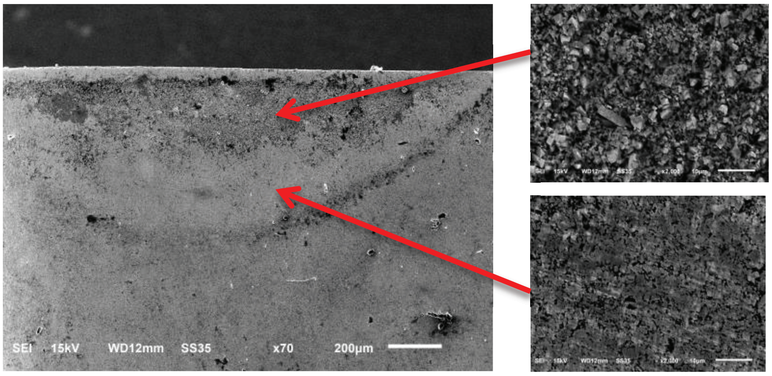

(a) Surface right underneath the Adhesion layer.

(b) Surface near the wear front showing some abrasion marks.

Figure 6: Etched Uncoated carbide insert after cutting CGI at 100 m/min for 10 min

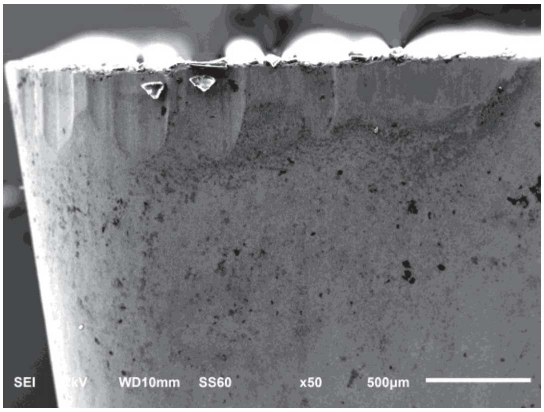

Figure 7: Flank wear surface after cutting FGI at 250 m/min for 1 min and 30 sec showing no adhesion layer formation.

Figures 8, 9 & 10 show the comparison in flank wear between FGI and CGI with the uncoated carbide inserts. Unexpectedly, flank wear on FGI is much more extensive than that of CGI for all three cutting speeds. Philip (1981) is the only publication reporting the turning experiment with uncoated carbides. Despite no details was given, he has also observed the better tool life with uncoated carbide. This does not agree well with the results with uncoated carbides from the milling experiment (Abel et al., 2002). So far no one reported the layers formed on flank observed in Figure 2. Our experiments with CGI consistently had the adhesion layers on every uncoated inserts except some at high cutting speeds. This adhesion layer seems to protect the flank surface. With the coated inserts, no such layer was found and the flank wear become more severe with CGI as expected. The flank wear results for both multilayered coated carbide inserts, Sandvik 3205 and 3210, are presented in Figure 9 with the modest improvement with Sandvik 3210. This is believed to be the presence of thicker and harder Ti(C,N) layer which resist abrasive wear as presented in Table 4. As illustrated in Figure 10, the flank wear comparison between uncoated and coated inserts at the cutting speed of 250m/min is also striking.

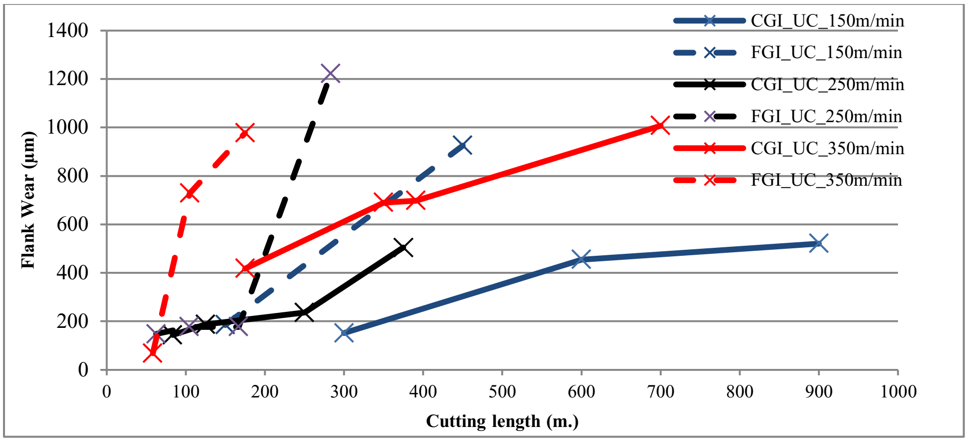

Figure 8: Comparison the flank wear after cutting FGI and CGI with uncoated carbide inserts at 150, 250 and 350 m/min)

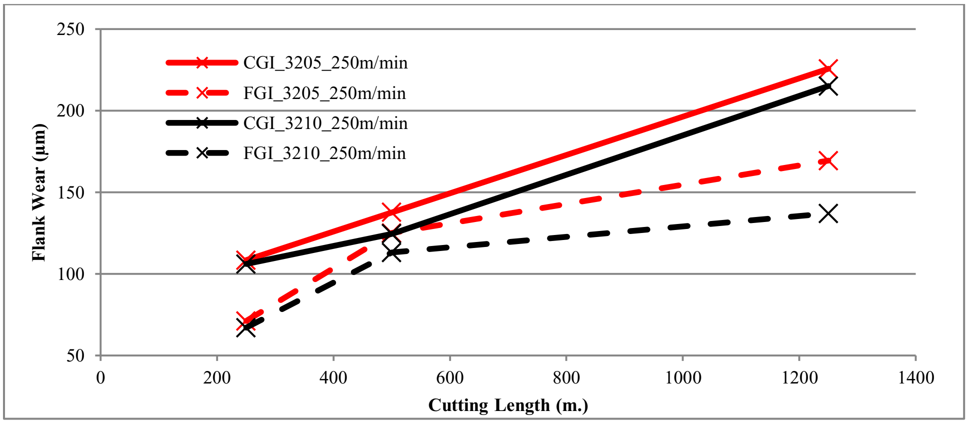

Figure 9: Comparison the flank wear after cutting FGI and CGI with the multilayer coated carbide inserts at 250 m/min

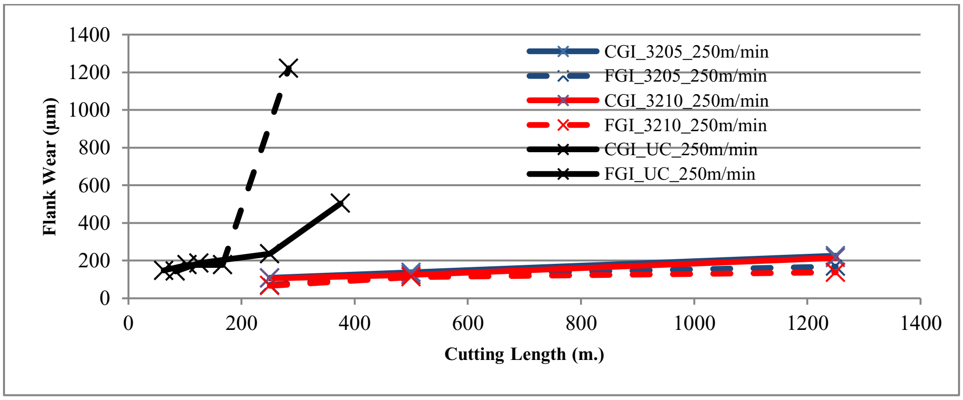

Figure 10: Comparison the flank wear of FGI vs. CGI (Multilayer coated and uncoated carbide inserts at 250 m/min)

3.2 Crater Wear

The wear mechanisms are know to be a combination of abrasive and dissolution/diffusion wear. Some adhesions on the rake face of the insert were presented after machined CGI and FGI as shown in Figures 11 and 12. However, the morphology of the adhesion layer is completely distinct. After machining CGI, the adhesion occurs right at the cutting edge, which was identified to be mostly Fe and W and C from the carbides using EDS (shown in Figure 11). Machining FGI produces patches of adhesion layers as shown in Figure 12. Pereira et al. (2006) also reported the adherence of work material (FC25) on uncoated carbide tools. This adhesion occurred when sulfur content in work material was less than 0.065% or the area occupied by MnS was lower than $(18\pm6)\times10^{-3}$. The back-scattered electron detector (BSE) image shows some adhesion of iron, detected and confirmed by energy dispersive X-ray spectroscopy (EDS) adhered on the rake face of cutting insert near the cutting edge.

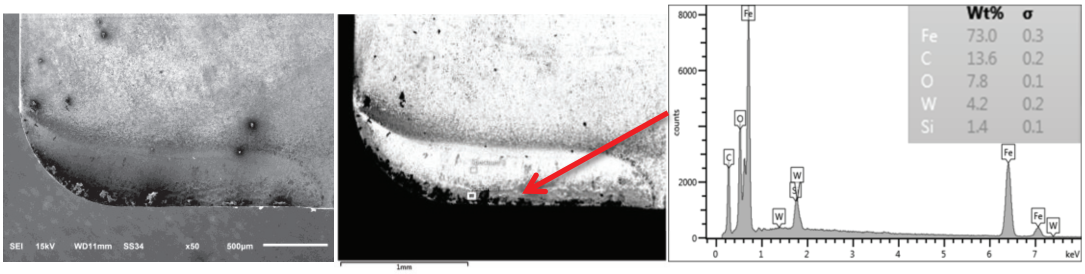

(a) **(b)** **(c)**

Figure 11: SEI (a), BSE (b) and EDS (c) on the rake face of uncoated carbide insert after cutting CGI at 150 m/min for two mins.

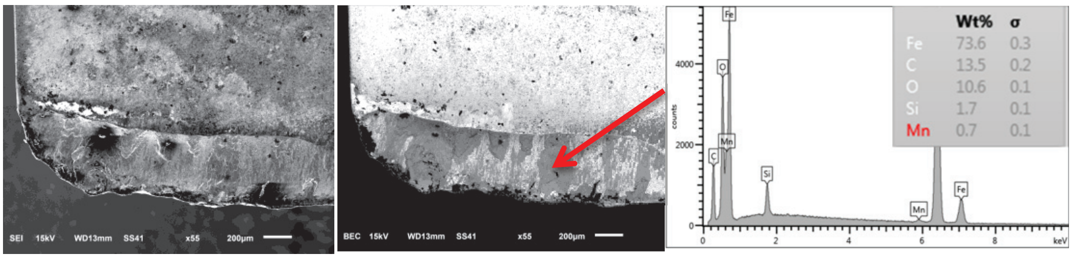

(a) **(b)** **(c)**

Figure 12: SEI (a), BSE (b) and EDS (c) on the rake face of uncoated carbide insert after cutting FGI at 250 m/min for 50 sec.

Figures 13, 14 & 15 show the comparison of the crater wear evolution between FGI and CGI with uncoated carbide inserts. Crater wear on FGI is much more extensive (up to 6 times) than that of CGI for all three cutting speeds. As observed with more flank wear with FGI, more crater wear was observed, which is totally unexpected. The crater wear after turning CGI expected to retain higher wear because of the superior in physical and mechanical properties of CGI (Dawson et al. 2001) and also higher cutting temperature generated during the machining of CGI. (Mohammed et al. 2012) Mostly smooth wear profiles, which are the main indicative feature of dissolution wear in ferrous materials (Kim et al., 2001), were seen on the rake face of the tools. However, the crater wear on FGI is not as even compared to those of CGI. The patches of damages can be seen as similarly observed on the flank wear of FGI. In FGI, the inhomogeneity in the cast iron is more prevalent and, as the cutting continues, the damage accumulates.

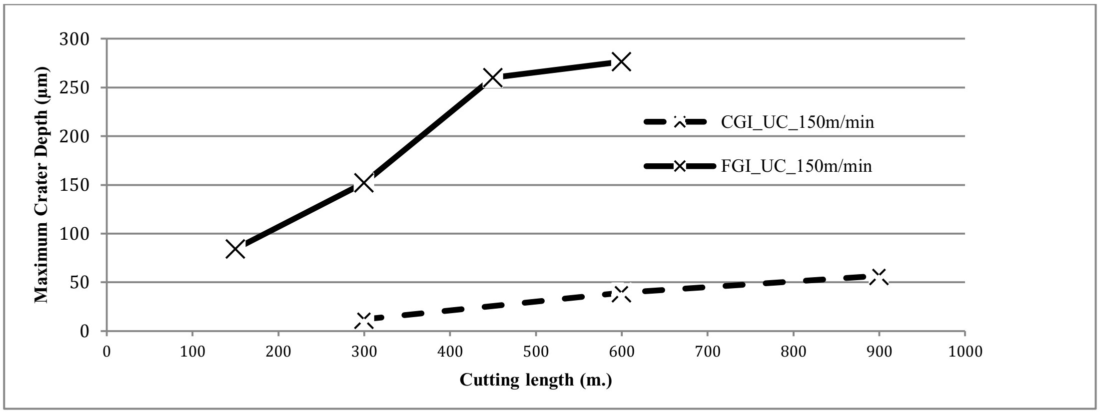

Figure 13: Comparison the crater wear of FGI vs. CGI (Uncoated carbide inserts at 150 m/min)

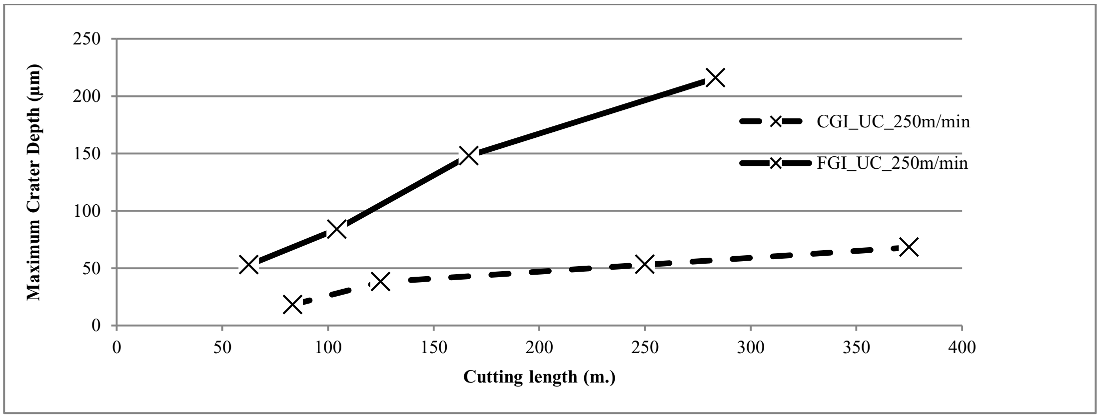

Figure 14: Comparison the crater wear of FGI vs. CGI (Uncoated carbide inserts at 250 m/min)

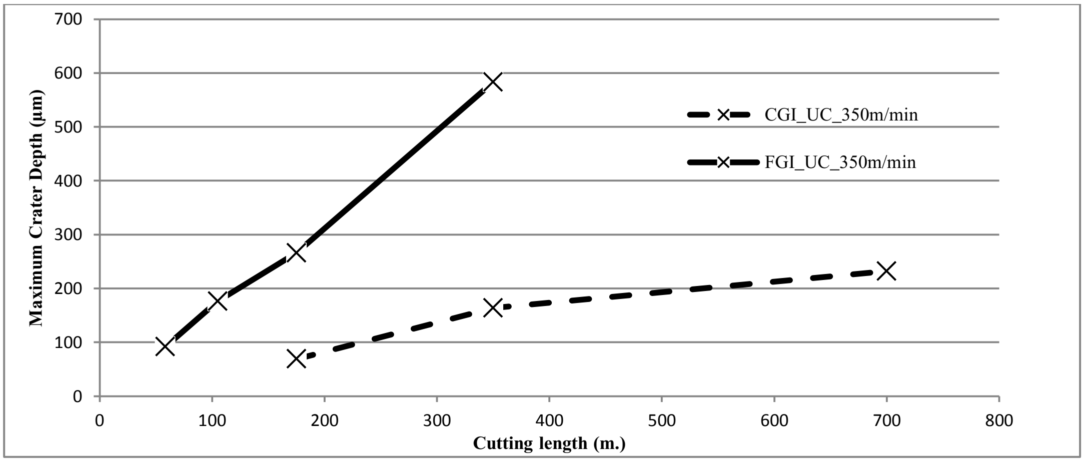

Figure 15: Comparison the crater wear of FGI vs. CGI (Uncoated carbide inserts at 350 m/min)

The multilayer coated carbide inserts used in this experiments have two layers, Ti(C, N) and Al_2O_3 (exterior coating) with the additional thin (1-2 microns) layer of TiN coating on the flank surface had on the surface provided substantially better performance comparing with the uncoated carbide inserts. Al_2O_3 is the dissolution resistant coating while Ti(C, N) is the abrasive resistant coating material. (Wong et al., 2006) The combination of these coating materials comprehensively increases the wear resistance. The hairline cracks on the surface are very common for multilayer coated inserts due to the process-induced residual stress. However, the delamination or detachment of any segment of coatings is not common. Figure 16 shows the smooth macroscopic texture of the crater wear with the shallow grooves in the chip flow direction indicating abrasive wear. Figure 17 also illustrated the same insert after 9 more minutes of cutting with the smooth texture observed in Figure 16 with much more defined abrasive marking as the softer carbide substrate is exposed.

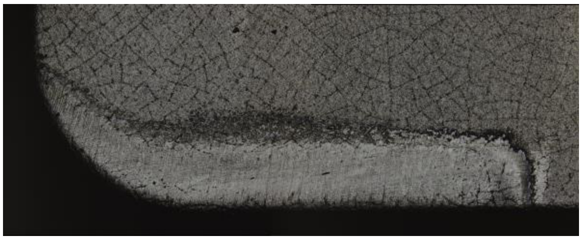

Figure 16: Optical image of crater wear after cutting FGI at 250m/min for one minute with the multilayer coated carbide insert (3210).

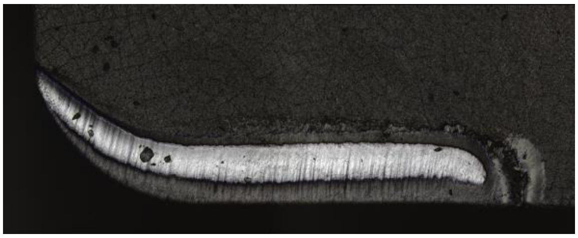

Figure 17: Optical image of crater wear after cutting FGI at 250m/min for ten minutes with the multilayer coated carbide insert (3210).

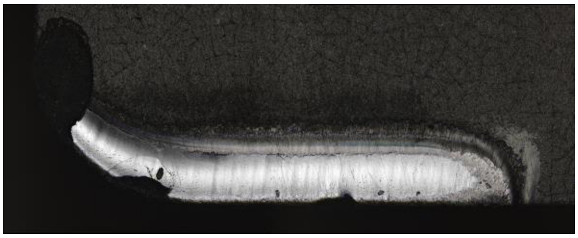

Figure 18: Optical image showed the evidence of few chippings on the multilayer coated carbide insert (3210) after cutting CGI at 250 m/min for 10 min.

Figure 19 shows the comparison of crater wear retained after turning CGI and FGI with the multilayered coated inserts. The crater wear attained with CGI is comparable to that attained with FGI. This result agrees with the investigation of Nayyar et al. (2012) which presents a slightly better tool life with FGI compared to CGI and also indicated some adhesion on the rake face without any detailed information. Figure 20 demonstrate the effectiveness of the multilayer coated carbide inserts which a provided significantly higher performance compared to the uncoated carbide inserts for both FGI and CGI.

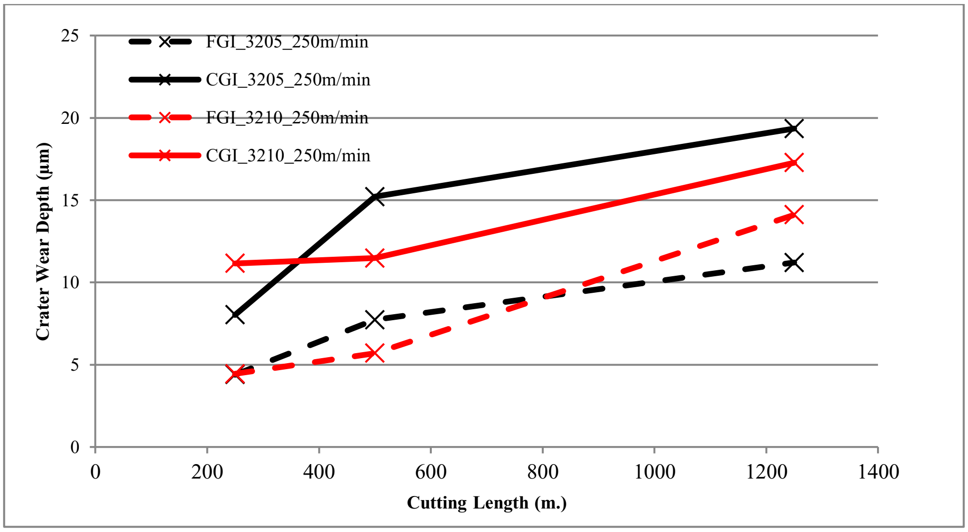

Figure 19: Comparison the crater wear of the multilayer coated carbide inserts between FGI and CGI after cutting at 250 m/min

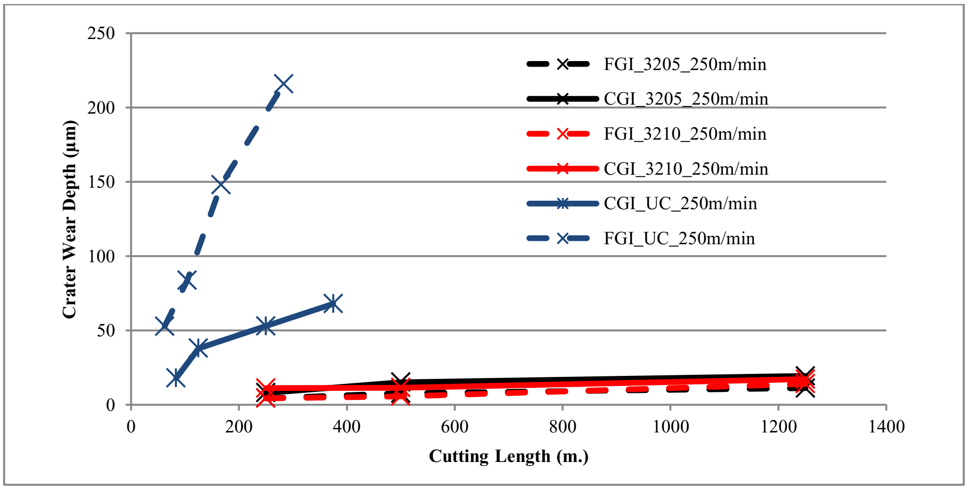

Figure 20: Comparison of the crater wear between uncoated and multilayer coated carbide inserts.

4 Conclusion

A preliminary machining study was conducted on FGI and CGI with uncoated and multi-layer coated carbide inserts. Obviously the tool lives of the coated inserts were much higher than those of the uncoated inserts for both FGI and CGI as evident in Figure 10. However, it has been established that the machinability of CGI is considered to be poor compared to that of FGI. Gastel et al. (2000) has concluded that the presence of MnS, when turning FGI at extremely high cutting speed (above 600m/min) only possible with PCBN inserts, provides the lubricity and thus the excellent machinability of FGI. This study concentrated on the machinability in the conditions ideal for carbide and coated carbide inserts. Surprisingly, with the uncoated inserts, the machinability of CGI is better than FGI contradicting the report (Dawson et al., 2001). This is contributed by the unexpected adhesion layer on the flank side and the cutting edge of rake face of carbide inserts observed on the uncoated carbide inserts when turning CGI. This adhesion layer is believed to protect the flank and rake surfaces and reduce tool wear. Flank wear land is mostly covered by the adhesion layer while the adhesion layer is formed only at the cutting edge of rake faces when turning CGI. As the cutting continues, the adhesion layers eventually dissipate as the scoring marks dominate the flank surface. In contrast, the adhesion layer was rarely present when turning FGI at low cutting speed. Even if the adhesion layer was present, it does not stay for an extended period of cutting and much more extensive tool wear – both flank and crater wear – is inevitable on the uncoated carbide inserts. However, when multilayer-coated tools are used to cut FGI and CGI, no such adhesion layer was formed and CGI produced more extensive flank and crater wear as reported elsewhere (Dawson et al., 2001).

5 Acknowledgement

This work has been supported by Korea Institute of Industrial Technology (KITECH, JA-15-0034) and the Ministry of Knowledge Economy (MKE) in Republic of Korea (Project title is “Development of liquid nitrogen based cryogenic machining technology and system for titanium and CGI machining”, 10048871). We also acknowledge Mr. Brian Hoefler at Sandvik Coromant providing the inserts for this study.

References

Abele, E., Sahm, A. and Schulz, H., 2002. Wear mechanism when machining compacted graphite iron. CIRP Annals-Manufacturing Technology. 51(1). pp.53-56.

Dawson, S., 1999. Compacted graphite iron: mechanical and physical properties for engine design. Vdi Berichte, 1472. pp.85-106.

Dawson, S. and Schroeder, T., 2000. Compacted graphite iron: a viable alternative. Engineering Casting Solutions AFS.

Dawson, S., Hollinger, I., Robbins, M., Daeth, J., Reuter, U. and Schulz, H., 2001. The effect of metallurgical variables on the machinability of compacted graphite iron (No. 2001-01-0409). SAE Technical Paper.

Dawson, S. and Schroeder, T., 2004. Practical applications for compacted graphite iron. AFS Transactions. 47(5). pp. 1-9.

Gastel, M., Konetschny, C., Reuter, U., Fasel, C., Schulz, H. and Riedel, R., 2000. Investigation of the wear mechanism of cubic boron nitride tools used for the machining of compacted graphite iron and grey cast iron. International Journal of Refractory Metals and Hard Materials. 18. pp. 287- 296.

Heck, M., Ortner, H. M., Flege, S., Reuter, U. and Ensinger, W., 2008. Analytical investigations concerning the wear behaviour of cutting tools used for the machining of compacted graphite iron and grey cast iron. International Journal of Refractory Metals and Hard Materials. 26(3). pp. 197-206.

Kim, W. and Kwon, P., 2001. Understanding the mechanisms of crater wear. Transactions of NAMRI/SME (109). pp. 87-91.

Lalich, M. J. and LaPresta, S. J., 1977. Progress in the use of compacted graphite cast iron for engineering applications. ASM Materials Conference. Paper No. 32.

Mocellin, F., Melleras, E., Guesser, W. L. and Boehs, L., 2004. Study of the machinability compacted graphite iron for drilling process. Journal of the Brazilian Society of Mechanical Sciences and Engineering, 26(1). pp. 22-27.

Mohammed, W. M., Ng, E. and Elbestawi, M. A., 2012. Modeling the effect of compacted graphite iron microstructure on cutting forces and tool wear. CIRP Journal of Manufacturing Science and Technology. 5(2). pp. 87-101.

Nayyar, V., Kaminski, J., Kinnander, A. and Nyborg, L., 2012. An experimental investigation of machinability of graphitic cast iron grades; flake, compacted and spheroidal graphite iron in continuous machining operations. Procedia CIRP. 1. pp.488-493.

Nayyar, V., Grenmyr, G., Kaminski, J. and Nyborg, L., 2013. Machinability of compacted graphite iron (CGI) and flake graphite iron (FGI) with coated carbide. International Journal of Machining and Machinability of Materials. 13(1). pp. 67-90.

Oathout, R. R., 1978. Compacted graphite iron for diesel engine castings. Metal Progress. 113(5). pp. 54-57.

Pereira, A. A., Boehs, L. and Guesser, W. L., 2006. The influence of sulfur on the machinability gray cast iron FC25. Journal of Materials Processing Technology, 179(1). pp.165-171.

Phillips, C. W., 1982. Machinability of compacted graphite iron. (Retroactive Coverage). Transactions of the American Foundrymen's Society. 90. pp. 47-52.

Shen-Chih, L. E. E. and CHANG Yin-Bean., 1991. Fracture toughness and crack growth rate of ferritic and pearlitic compacted graphite cast iron at 25°C and 150°C. Metallurgical Transactions A 22. pp. 2645-2653.

Wong, T. K. and Kwon, P., 2006. Dissolution profile of tool material into chip lattice. Journal of Manufacturing Science and Engineering, 128(4). pp. 928-937.